Geometric Changes in a Tidewater Glacier in Svalbard during its Surge Cycle

Authors: Murray, Tavi, James, Timothy D., Macheret, Yuri, Lavrentiev, Ivan, Glazovsky, Andrey, et al.

Geometric Changes in a Tidewater Glacier in Svalbard during its Surge Cycle

Tavi Murray*‡

Timothy D. James*

Yuri Macheret†

Ivan Lavrentiev†

Andrey Glazovsky† and

Helena Sykes*

*Glaciology Group, Swansea University, Swansea, SA2 8PP, U.K.
†Institute of Geography, Russian Academy of Sciences, Staromonetny per., 29, Moscow 119017, Russia
‡Corresponding author: t.murray@swansea.ac.uk

Abstract

Fridtjovbreen, Svalbard, is a partially tidewater-terminating glacier that started a 7-year surge during the 1990s. Flow peaked during 1996 and no surge front was apparent. We use two pre-surge (1969 and 1990) and a post-surge (2005) digital elevation models (DEMs) together with a bed DEM to quantify volume changes and iceberg calving during the surge, calculate the changes in glacier hypsometry, and investigate the surge trigger. Between 1969 and 1990, the glacier lost 5% of its volume, retreated 530 m and thinned by up to 60 m in the lower elevations while thickening by up to 20 m in its higher elevations. During the surge, the reservoir zone thinned by up to 118 m and the receiving zone thickened by ~140 m. Fridtjovbreen's ice divide moved ~500 m, incorporating extra ice into its catchment. Despite this volume gain, during 1990–2005 the glacier lost ~10% of its volume through iceberg calving and 7% through surface melt. The surge occurred in a climate of decreasing overall ice volume, so we need to revise the notion that surging is triggered by a return to an original geometry, and we suggest Fridtjovbreen's surge was triggered by increasing shear stresses primarily caused by increases in surface slope.

Introduction

A surge-type glacier cycles between long periods of slow flow (quiescence) and short periods of fast flow (surge), during which ice flow speed may accelerate by over an order of magnitude (e.g., Cuffey and Paterson, 2010). During the quiescent phase, ice flow rates are slower than the balance velocity, and mass builds up in the upper part of the glacier; simultaneously, the lower part of the glacier thins and the glacier consequently steepens overall. The front margin of the glacier often also retreats. During the surge, fast flow results in transport of ice downglacier at rates above the balance velocity, often accompanied by an advance of the glacier front margin. Thus a surge-type glacier is viewed as cycling between two end member geometries, with the extremes occurring immediately pre- and post-surge. In his description of this dynamic and geometric cycle, Raymond (1987) stated that thickness changes during quiescence ''reverse the thickness changes of the surge and gradually return the glacier to near its presurge state''; van der Veen (1999) stated that surging starts when a ''glacier reaches a certain thickness'', and Cuffey and Paterson (2010) when a ''glacier attains some critical profile.'' There thus seems to be considerable agreement in the literature that we should expect glaciers to return to a pre-surge geometry prior to a subsequent surge.

Remote sensing techniques, such as satellite radar interferometry and cross-correlation tracking, have led to considerable knowledge of the changing ice dynamics through the active phase of glacier surging in Svalbard (Luckman et al., 2002; Strozzi et al., 2002; Murray et al., 2003a, 2003b; Mansell et al., 2012). Synthesis of remote sensing results with those from field methods suggests two types of surges occur in Svalbard (Murray et al., 2003b). During surges of land-terminating glaciers, typified by the surge of Bakaninbreen (Murray et al., 1998), fast flow appears to initiate in the reservoir zone and a surge front propagates downglacier, in a manner similar to that observed at Variegated Glacier, Alaska (Kamb et al., 1985). In contrast, during surges of tidewater-terminating glaciers, fast flow appears to initiate low down and spread both up and downglacier (Pritchard et al., 2005). In Svalbard, this type of surge is typified by the surge of Monacobreen (Luckman et al., 2002; Murray et al., 2003b). The two types of surge form distinct crevasse and structural patterns because the passage of a surge front downglacier is characterized initially by compression (typically forming longitudinal crevasses) followed by extension (forming transverse crevasses) as the front passes (Murray et al., 1998). If no surge front forms or in regions of the glacier that experience only extensive flow regimes only transverse crevasses will occur.

Remote sensing techniques also allow mapping of the changing morphology of a glacier surface in 3-D during a glacier surge. Such studies have been undertaken in a variety of environments including Greenland (Jiskoot et al., 2001; Pritchard et al., 2003) and Alaska (Muskett et al., 2008, 2009; Shugar et al., 2010). In Svalbard an analysis of repeated ASTER digital elevation models (DEMs) was used to suggest a long initiation phase, with mass being transferred downglacier slowly causing deflation of the surface at high elevations prior to the fast flow event (Sund et al., 2009). In this paper we use photogrammetry and airborne lidar to produce three surface DEMs covering the full surface area of Fridtjovbreen, Svalbard. Fridtjovbreen is a partially tidewater-terminating glacier at which fast flow during the surge started low down on the glacier (Murray et al., 2003a). Our DEMs cover both late quiescence and postsurge, and therefore for the first time for a Svalbard surge, bracket the full active phase. We use these DEMs to quantify the redistribution of ice and iceberg calving, and to calculate the changes in glacier hypsometry and to investigate the surge trigger.
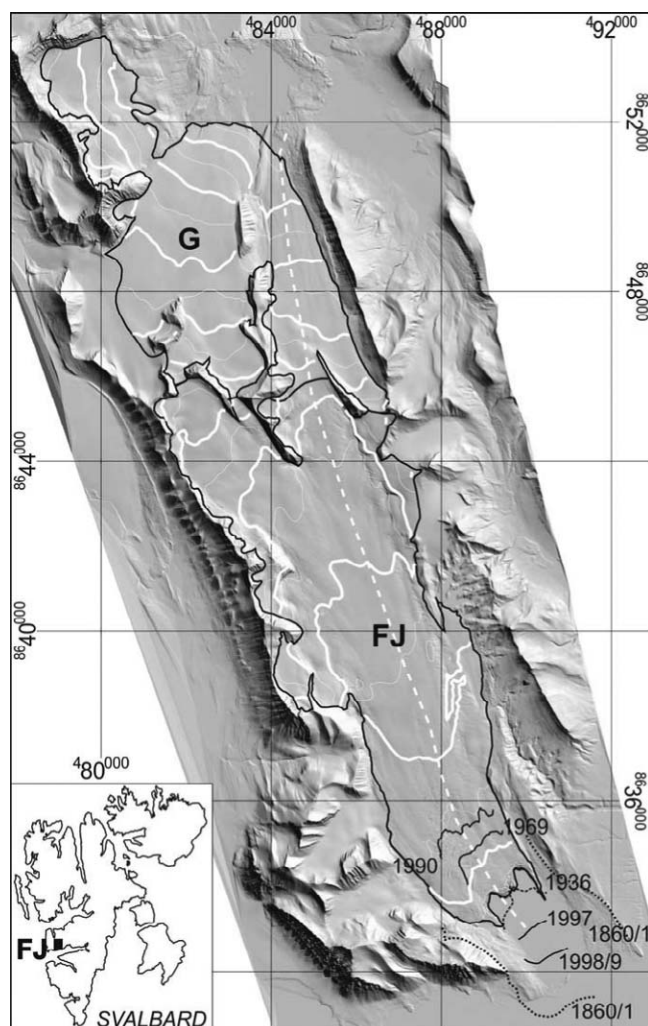
FIGURE 1. Shaded relief DEM from 2005 of Fridtjovbreen (FJ) and Grønfjordbreen (G) from lidar data. Contours are spaced at 50 m intervals, heavy white contours at 100 m. Coordinates are UTM coordinates (zone 33X) in meters (ellipsoid WGS84). Black line delineates the 2005 glacier boundary. Dashed white line is profile shown in Figure 4. Insert shows location of FJ within Svalbard. Additional margin positions are shown from 1990 and 1969 (aerial photographs), 1997, 1998/1999 from maps and reconstructed 1860/1861 margin from Lønne (2006).

Study Area

Fridtjovbreen, Svalbard (Fig. 1; 77°50′N, 14°26′E) is a 13-km-long surge-type glacier with an area of ∼38 km². The glacier flows southwards from an ice divide with the non-surge-type glacier, Grønfjordbreen. Fridtjovbreen flows towards van Mijenfjord, which trends east-west, approximately perpendicular to Fridtjovbreen's flow. Fridtjovbreen varies in width from ∼5 km to ∼1.5 km near its front margin. Radio-echo sounding shows the glacier is polythermal over most of its length. A cold surface layer of thickness ∼100 m overlies warm ice up to 220 m thick (Macheret and Glazovsky, 2000). This thermal structure was confirmed by two deep boreholes (Kotlyakov and Macheret, 1987). Fridtjovbreen is one of a small number of glaciers in Svalbard where multiple surges have been observed (Mansell et al., 2012): one occurred ca. 1860–1861 (Hagen et al., 1993), a possible surge event in ca. 1898

(see discussion below), and one which began in 1995 (Murray et al., 2003a).

During 1858 Fridtjovbreen was visited by Torell's expedition and was clearly in quiescence, with its terminus situated inland of Fridtjovhamna (harbor), separated from the fjord by a ''marsh'' (Liljequist, 1993). However, by winter 1860–1861 Nordenskiold's expedition found that the ''once small glacier had expanded across the moraines before it in the harbour's interior; it had then filled the entire harbour and even passed beyond'' (Liljequist, 1993). At that time the terminus almost reached Axelsøya, a rock bar at the mouth of van Mijenfjord (Hjelle et al., 1986). We interpret the glacier to have surged ca. 1860–1861 from these descriptions (see inferred marginal position from Lønne [2006] on Fig. 1).

Six years later in 1866, maps produced by Nordenskiold show the glacier terminating well inland (Glasser et al., 1998). A subsequent map of 1898 by Kyellström and Hamberg again shows the glacier beyond the confines of Fridtjovhamna (in Nathorst, 1900). However, by 1909, the glacier surface was described as smooth and uncrevassed (Glasser et al., 1998). This report of the front margin again outside the harbor in 1898 suggests a previously unreported surge event may have occurred at the end of the 19th century.

Subsequently for the majority of the 20th century, the glacier continued to retreat, displaying a pattern of low-elevation thinning and high-elevation thickening typical of a surge-type glacier in quiescence. For example, between 1936 and 1988, the front margin retreated by ∼1.3–2 km, and thinned by ∼100 m (Glazovsky et al., 1991). Over the same time period, the glacier thickened at elevations higher than 350 m a.s.l., with the northwestern (NW) tributary thickening by ∼40 m (0.8 m a⁻¹) and the northeastern (NE) tributary by ∼10 m (0.2 m a⁻¹). During the early 1990s, the western side of the front margin was tidewater-terminating, forming a cliff, whereas the eastern side terminated on land (Musial, 1994). The majority of the ice surface was crevasse-free.

The dynamics of the 1990s surge was studied using satellite radar interferometry (Murray et al., 2003a). The glacier underwent a slow acceleration between 1991 and June 1995, with flow rates exceeding the balance velocity throughout. Fast flow started in the lower third of the glacier (Murray et al., 2003a). The trunk and NW tributaries moved faster than the NE tributary. The glacier surface changed, with intermittent lakes and increased transverse crevassing (Musial, 1994). The glacier front remained static until at least March 1994; however, by October 1995 the glacier had advanced 350 m. Between June 1995 and February 1996, the glacier accelerated rapidly, reaching a measured maximum ice flow speed of 2.5 m d⁻¹. By May 1997, the glacier front had advanced ∼2.8 km from its pre-surge location at peak rates of 4.2 m d⁻¹ and its margin became intensely chaotically crevassed. The next measurement in October 1997 showed flow rates had begun to decrease and the margin had begun to retreat (Murray et al., 2003a), however, Lønne (2006) reports subsequent re-advance of ∼650 m with maximum frontal extent in 1998/1999. The maximum frontal position was less advanced than that of 1860–1861 (Fig. 1). Bamber et al. (2005) reported thinning of −0.26 m a⁻¹ along a single flowline on Fridtjovbreen between 1996 and 2002, but these measurements were made after the main advance had occurred and are not comparable either in technique or timeframe with the measurements we present in this paper.

Field observations suggested that the fast-flow phase of the 1990s surge started near the terminus (A. J. Hodson, personal communication, 2002) and propagated up-glacier, initially to the NW tributary in agreement with flow speeds. The initiation zone for fast flow is corroborated by surface crevasses on the upper glacier, which were exclusively transverse (Murray et al., 2003a), suggesting only extension had occurred in this region as well as the remote sensing observations described above. Drawdown in the reservoir zone was visually estimated to be ~10 m (A. J. Hodson, personal communication, 2002), although in this paper we show it was actually much greater. No surge front was observed during the fast flow phase in the field, on satellite images or on interferograms, and the 1990s surge of Fridtjovbreen appears to fit the characteristics of a tidewater-terminating glacier surge.

Methods

SURFACE DEMS

A lidar DEM was collected in July 2005 over the Fridtjovbreen and Grønfjordbreen catchments by the U.K. Natural Environment Research Council's (NERC) Airborne Research and Survey Facility (ARSF) using an airborne Optech Airborne Laser Terrain Mapper (ALTM) 3033 system. This instrument records the timing of the first pulse, last pulse, and 8-bit laser intensity data for each observation. A Global Positioning System (GPS) base station was run at Finsterwalderbreen, ~30–45 km from Fridtjovbreen, and these data were combined with: (i) the laser range data; (ii) GPS mounted on the aircraft; and (iii) Inertial Navigation System (INS) measurement of aircraft attitude (pitch, roll, and yaw) in post-processing to produce a data cloud of (X, Y, Z, intensity) data. The lidar data set consisted of over 150 million data points with an average spatial resolution of ~1 point per 1.67 m^2. The data are of sufficient quality and spatial resolution that both surface crevasses and supraglacial channels can be identified on the glacier surface (Fig. 1).

Topographic data were also derived from 1969 panchromatic (1:20,000) and 1990 color infrared (1:50,000) vertical aerial photographs from the Norwegian Polar Institute, which were captured using calibrated metric cameras. All of the images were collected in summer (July or August). Photogrammetric-quality scanning was undertaken at resolutions of 12.5 and 10 μm for the 1969 and 1990 photographs, respectively. The photogrammetric models were controlled using 67 ground control points located on geologically stable surfaces extracted from the lidar data (James et al., 2006; Barrand et al., 2009). Where the automated stereo-image correlation failed (i.e. in steep or snow-covered areas), points were collected manually wherever surface texture allowed. Both photogrammetric DEMs were collected with a point spacing of 20 m.

The three surface DEMs bracket the fast flow phase of Fridtjovbreen's 1990s surge. The period between the 1969 and 1990 photogrammetric DEMs covers 21 years of late quiescence, whereas the period between 1990 and 2005 covers the active phase of the surge.

Volume changes between epochs were calculated by differencing the surface DEMs. To isolate ice-covered areas, ice mask polygons were constructed for each epoch from the aerial photography. The relevant masks were combined to capture the largest ice area for each period. However, since Fridtjovbreen is tidewater-terminating, the volume of ice stored or lost between successive ice margin positions also requires knowledge of the fjord bottom bathymetry, which is discussed below.

The hypsometry of a glacier is the area-elevation distribution. Hypsometry is controlled by factors such as valley shape and topographic relief, and is thought to be a factor that may contribute to whether a glacier has normal, stable flow or exhibits unstable, surge behavior. In Alaska a glacier that is 'bottom heavy' has been suggested to be more likely to be of surge-type (Wilbur, 1988); however, no such relationship was found in Svalbard (Jiskoot et al., 2000). We therefore calculate and present the hypsometry of Fridtjovbreen both before and after its surge.

SURFACE DEM AND VOLUME CHANGE ERROR ASSESSMENT

The remote nature of Fridtjovbreen meant it was not possible to collect ground-truth data at the glacier simultaneously with lidar data collection, but such data were acquired at several more accessible sites around Svalbard. These data included points close to the main GPS base station (i.e., over the airport runway), as well as two sites further afield with baseline lengths of similar distance as the Fridtjovbreen site. Those data were used to provide a robust assessment of the quality of the lidar data collection and post-processing. The results show mean elevation differences on glaciated regions of 0.14 m (Barrand et al., 2009).

The quality of the photogrammetrically derived surface DEMs was assessed in two ways. First, the root-mean-square (RMS) errors of the block adjustments provided an indication of the degree to which the block adjustments conformed to measured parameters and their specified precisions (Table 1). Second, a small area of each DEM (3500 pixels), which was geologically stable, and had similar contrast and slope to the glacier surface, was compared to the 2005 lidar DEM. This approach provided a means of assessing the quality of the image correlation stage of the photogrammetry in the absence of local ground-truth data. The results show mean errors of 1 m or less with standard deviations better than 1.4 m (Table 2). Errors in the difference DEMs can be calculated using standard error theory, which gives ~1.8 m and ~1.4 m in the pre and post-surge difference DEMs, respectively. These errors are evaluated for good contrast areas, and are the values we use in the area of the glacier which consists of bare ice in the photographs. In regions of the difference DEM where the contrast is lower due to snow cover we take a more conservative error estimate of 2 m. These estimates are then propagated to estimate errors in volume change which are quoted in Table 3.

BED DEM

We combined fjord sounding depths, photogrammetric heights of terrestrial margin areas, and radio-echo sounding (RES) data

TABLE 1
Block adjustment root-mean-square (RMS) errors (in meters).

	1969	1990
RMS error X	2.7	1.3
RMS error Y	3.4	1.3
RMS error Z	0.7	0.4
Image (pixels)	1.3	1.1

TABLE 2

Error statistics for the comparison of small regions of each photogrammetric digital elevation model (DEM) with the 2005 lidar DEM. Regions were selected to have stable characteristics and similar slopes to the glacier surface (in meters).

	2005–1969	2005–1990
Minimum	−5.8 m	−6.1 m
Maximum	9.2 m	7.5 m
Number of pixels	3232	3232
Mean	1.0 m	−0.3 m
Std Dev	1.2 m	1.4 m

(Fig. 2, part a) to create a bed DEM for the glacier. These data sets were interpolated into a 200 m DEM using an inverse distance weighting algorithm within ArcGIS (Fig. 2, part b).

The sounding depths were collected in 1984 and covered much of the fjord region between the 1990 and 2005 calving fronts of Fridtjovbreen (L. Christiansen, personal communication, 2007). The sounding depths are affected by systematic error related to the unknown height of the tide at the time of measurement, but this is small in Svalbard (~2 m tidal range; Norwegian Hydrographic Service, 1990). Radio-echo sounding (RES) at 2–13 MHz was undertaken at Fridtjovbreen in 1988 (Glazovsky et al., 1991). The survey consisted of 197 soundings over the relatively uncrevassed regions of the glacier (Fig. 2, part a). These soundings were converted to depths below surface using the results of a common-midpoint survey, which determined the mean velocity of electromagnetic wave (e.m.) propagation to be 0.169 ± 0.002 m ns^{-1}, and then to absolute elevation using the 1990 photogrammetric surface elevations.

The uncertainty in the radar depths are likely to be dominated by (i) error in the e.m. velocity used, especially given that Fridtjovbreen is polythermal and therefore e.m. propagation velocity will vary spatially; and (ii) by picking error, because of the low frequency of the radar transmission. The likely error is $\sim \pm 10$ m.

BASAL SHEAR STRESSES

We extracted profiles from the DEM and bed on an approximate flowline along the NE tributary (profile location shown in Fig. 1) to the front margin. These surface and bed profiles allow calculation of the basal shear stress using the method of Kamb and Echelmeyer (1986) which takes into account the effects of longitudinal stress gradients. Basal shear stress τ_B is calculated from:

$$\tau_B(x) = \frac{1}{2\ell h^{1/n}} \int_{-\infty}^{+\infty} \tau_L(x') h^{1/n}(x') \exp{-|x'-x|/\ell} dx', \quad (1)$$

where ℓ is the longitudinal coupling length (i.e. the length over which the effects of changes in ice thickness and surface slope are averaged), h is the ice thickness, τ_L is the local slope stress, n is the exponent in Glen's flow law, which we take equal to 3, and x is the distance coordinate along the glacier centerline. The ratio ℓ/h lies in the range 1.5–2.5 for valley glaciers (Kamb and Echelmeyer, 1986), thus we use ℓ equal to twice the ice thickness.

Results

The new bed DEM for Fridtjovbreen (Fig. 2) covers ~85% of the glacier bed of which ~5% lies below sea level. The crevasse pattern and the steep shape of the calving front suggests that much of the area where depths are unknown also lies below sea level. Individual basins of up to 50 m below sea level were revealed in similar locations as reported in Glazovsky et al. (1991), but overall the bed is less deep than was provisionally reported in that publication.

During the pre-surge period (Fig. 3, part a), the glacier retreated by ~530 m (25 m a^{-1}) and thinned by up to 60 m (2.9 m a^{-1}). The line delineating mass loss near the front margin from mass gain is at an elevation of ~310 m a.s.l. At elevations lower than this, the mean thinning rate was 0.7 ± 0.1 m a^{-1} (Table 3 summarizes the changes between the epochs), while at elevations above this the glacier thickened by up to 20 m (0.95 m a^{-1}) with a mean thickening rate of 0.04 ± 0.1 m a^{-1}. However, much of

TABLE 3

Summary of changes between DEMs and error estimates. In the early epoch we use the term ''reservoir zone'' to refer to the high elevation region above ~310 m a.s.l., which shows areas of minor mass gain, and receiving zone for the part of the glacier lying at elevations lower than this altitude, which is losing mass (Fig. 3, part a). In the later epoch (surge) we use the terms ''reservoir zone'' and ''receiving zone'' to describe the regions that lose and gain mass, respectively. The line delineating these zones during the surge is at an elevation of ~204 m a.s.l. (Fig. 3, part b). See text for discussion of areas A–C and Figure 3 for their locations.

| Pre-surge (1969–1990)	Area (m^2)	Mean thickness change (m)	Volume change (m^3)
Reservoir zone	24.8×10^6	1 ± 3	$20 \times 10^6 \pm 60 \times 10^6$
Receiving zone (excluding area A)	17.2×10^6	-15 ± 2	$-270 \times 10^6 \pm 30 \times 10^6$
Area A	0.6×10^6	-77 ± 2	$-50 \times 10^6 \pm 1 \times 10^6$
Total pre-surge	42.6×10^6		$-300 \times 10^6 \pm 70 \times 10^6$
Surge (1990–2005)			
Reservoir zone	34.4×10^6	-46 ± 2	$-1600 \times 10^6 \pm 70 \times 10^6$
Receiving zone (excluding area B and C)	7.0×10^6	36 ± 1	$260 \times 10^6 \pm 10 \times 10^6$
Area B	2.0×10^6	119 ± 1	$244 \times 10^6 \pm 3 \times 10^6$
Area C	3.0×10^6	56 ± 1	$170 \times 10^6 \pm 4 \times 10^6$
Receiving zone total	12.1×10^6		$670 \times 10^6 \pm 10 \times 10^6$
Total surge	46.5×10^6		$-930 \times 10^6 \pm 70 \times 10^6$
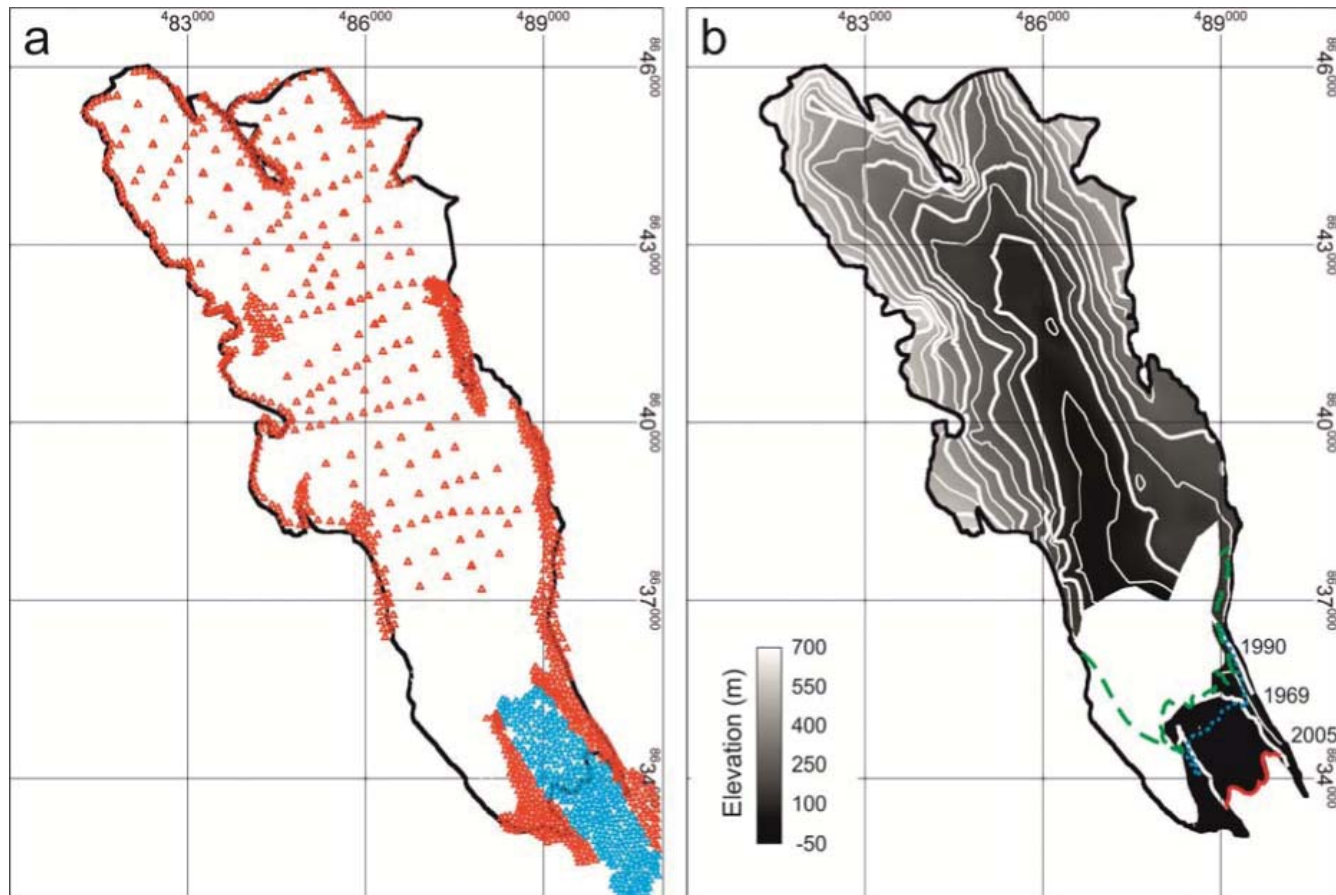
FIGURE 2. (a) Data locations (red points from radio echo-sounding and lidar/photogrammetry; blue points from bathymetric survey) for (b) bed DEM for Fridtjovbreen in m a.s.l. Contours are spaced at 50 m intervals. Coordinates are UTM coordinates (zone 33X) in meters (ellipsoid WGS84). Main text discusses data sources used in producing this DEM. White area shows region where no data exist because of heavy surface crevassing. Green dashed line is 1990 margin, blue dotted line is 1969 margin, and red line is 2005 margin.

the NW tributary lost mass over this period even at the highest elevations, and mass gain was largely limited to the upper and central parts of the NE tributary (Fig. 3, part a): a total volume of $2 \pm 6 \times 10^7$ m^3 was added to the glacier's reservoir zone. Ice margin retreat between 1969 and 1990 meant the glacier lost area of 9.4×10^5 m^2. This retreat showed the glacier had been partially land- and partially tidewater-terminating. The exposed bed above sea level could be measured from the 1990 DEM and had maximum elevation of ~65 m. Fjord depths where the glacier was tidewater-terminating between the two margin positions are reasonably well known (Fig. 2), and range between 0 and 39 m below sea level. Combining the bed and surface topography in this frontal region shows 5.0×10^7 m^3 of ice were lost due to marginal retreat over the fjord (region A in Fig. 3, part a) together with 27×10^7 m^3 of ice from the rest of the lower glacier. Overall the glacier lost volume equal to $30 \pm 7 \times 10^7$ m^3 during these 21 years, which is ~5% of the total glacier volume, equivalent to 0.33 m a^{-1} averaged over the whole glacier surface.

The glacier front was ~1800 m further advanced in 2005 than in 1990 (Figs. 1 and 3, part b), although some retreat had already occurred and, as discussed above, this position does not represent the maximum extent during the surge. The reservoir zone thinned by a maximum of 118 m (mean 46 ± 2 m), and the receiving zone had thickened by a maximum of 140 m (mean of 36 ± 1 m).

These thickness change values exclude the area of the ice advance between the 1990 and 2005 margin, where the average ice elevation is 110 m a.s.l. Combining the surface and bed DEMs, the volume stored by ice advancing in areas with elevations below sea level (area B in Fig. 3, part b) and above sea level (area C) was 41×10^7 m^3 (Table 3 summarizes the changes and gives error estimates). Overall the glacier lost 93×10^7 m^3 of ice during this 15 year period, equivalent to 17.2% of the glacier volume, or a thinning rate of 1.33 m a^{-1} averaged over the entire glacier surface. The line delineating mass loss (reservoir zone) and mass gain (receiving zone) lay at ~204 m a.s.l. (Fig. 3, part b), somewhat lower on the glacier than the equivalent line in the earlier epoch (Fig. 3, part a), and much better defined. At the highest elevations in the NE tributary, the catchment of Fridtjovbreen expanded during the surge to capture some ice that was previously within the Grønfjordbreen catchment (compare Fig. 3, parts a and b). This change in the size of the glaciers' catchments can also be seen in topographic profiles (Fig. 4, part a). These profiles highlight the changes in the surge-type Fridtjovbreen in contrast to its neighbor Grønfjordbreen.

To estimate the volume of icebergs calved during the surge we compare the overall thinning rates of Fridtjovbreen (-0.33 m a^{-1}) and Grønfjordbreen (-0.74 m a^{-1}) in the first pre-surge epoch (1969–1990) and assume that the ratio of the thinning rates due to melt between the glaciers in the second epoch (1990–2005)

TAVI MURRAY ET AL. / 363
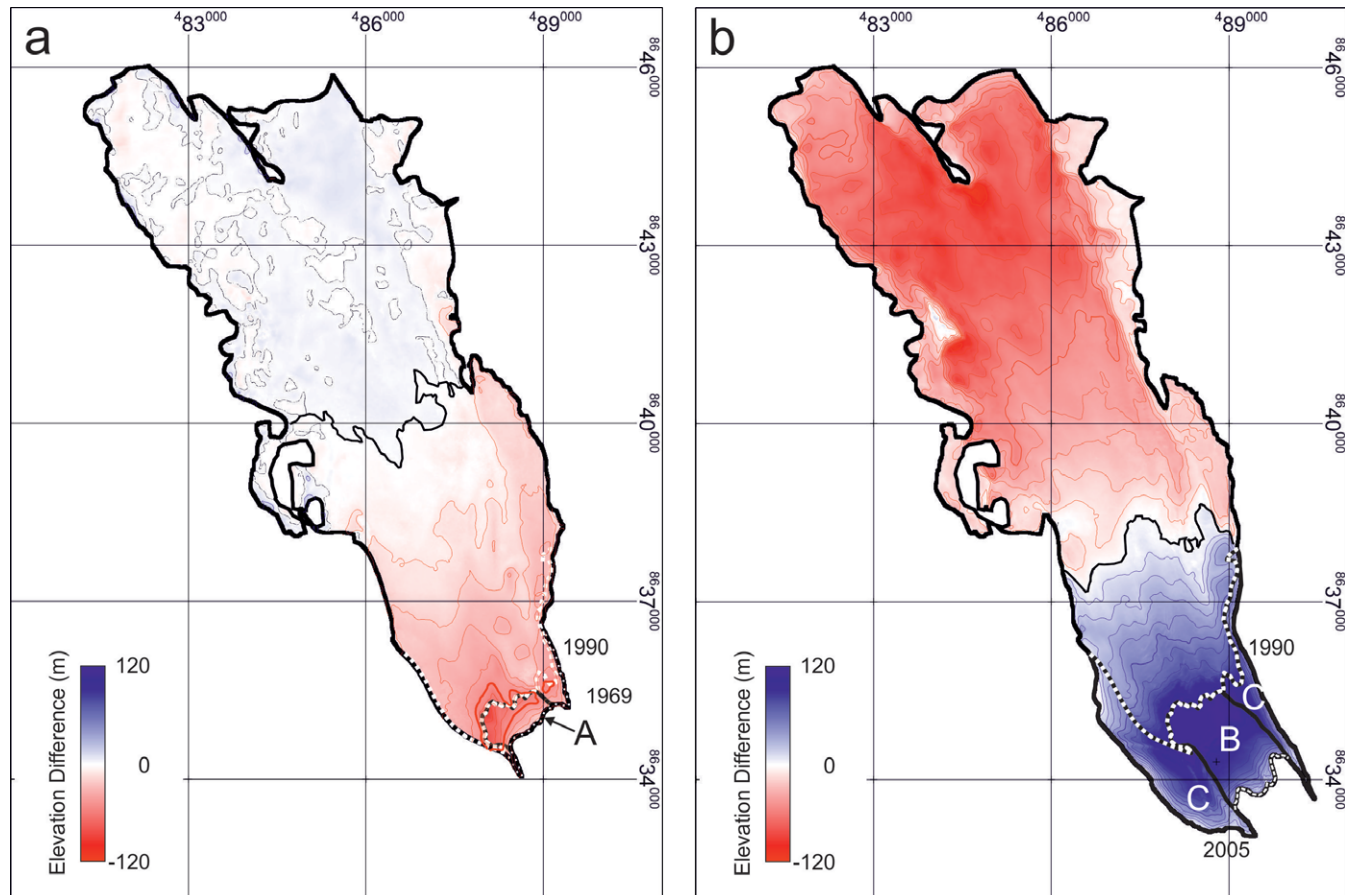
FIGURE 3. (a) Pre-surge difference DEM (1969 to 1990). Line shows approximate delineation between reservoir zone and receiving zone, although not all areas within the reservoir zone thickened. Maximum thickening ~20 m occurred in the NE tributary. Area A is region where glacial retreat exposed fjord water, so the volume change in this area is less well known because of limitations of the bed DEM. (b) Post-surge difference DEM (1990 to 2005). The DEM shows the effects of the glacier surge. Line shows delineation between reservoir zone and receiving zone (note that this is at a different location and elevation to the equivalent line in (a); see text for details). Area B is region where advance was into fjord water, so the volume change in this area is less well known because of limitations of the bed DEM. Areas C are regions where advance was over sediments or the tributary glacier Sagabreen (on west side). In both parts of this figure coordinates are UTM coordinates (zone 33X) in meters (ellipsoid WGS84). Contours of elevation change are at 10 m spacing, contours at 50 m spacing are thicker: red for mass loss, blue for mass gain. Zero change contour is black dashed line.

is the same. Using this ratio and the thinning rate of Grønfjordbreen in the second epoch (-0.53 m a^{-1}), we estimate the mass loss of Fridtjovbreen due to melting was ~37×10^7 m^3. Thus ~56×10^7 m^3 (equivalent to a thinning rate of 0.81 m a^{-1} averaged over the whole glacier surface) was most likely calved as icebergs into the fjord. This volume of calved ice represents ~10.4% of the total glacier volume.

The greatest changes in basal shear stress occur during the surge (Fig. 4, part b), between the 1990 and 2005 epochs, when basal shear stresses decrease in the reservoir zone and increase in the receiving zone due mainly to the large thickness changes. In the earlier epoch, during the buildup to fast flow (1969–1990), shear stresses increase over most of the lower glacier whereas stresses in the upper glacier show no change or decreasing shear stress during this period.

Figure 5 shows the hypsometry of Fridtjovbreen calculated at each of the DEM epochs. The hypsometric curves have essentially the same shape in both 1969 and 1990, reflecting a small amount of mass gain at elevations mainly between 450 and 500 m a.s.l. on

the NE tributary; however, there is a small mass gain at all elevation bands above this in addition, so there is no support for this period representing a period of mass transport downglacier as described by Sund et al. (2009). Rather the eastern side of the glacier thickened slightly and the western side thinned (Fig. 3, part a).

The surge caused transfer of mass downglacier, resulting in a large areal increase in the region of the glacier between 200 and 400 m a.s.l. In 1969, 61% of the glacier's area lay at elevations above the 1969–1990 measured reservoir-receiving line altitude, and by 1990 this had increased to 64%. After the surge, however, only 43% of the glacier's area lay above this altitude. Furthermore, comparison with measurements on neighboring non-surge-type glaciers show the equilibrium line altitude (ELA) is much higher during this period. For example, on Slakbreen the ELA has been at around 750 m a.s.l. since 1961 (Kohler et al., 2007). It is normally assumed that for a glacier to be in equilibrium, its accumulation area should comprise around 70% of the total glacier area (Cuffey and Paterson, 2010), so that overall mass loss from Fridtjovbreen in both epochs is not unexpected.
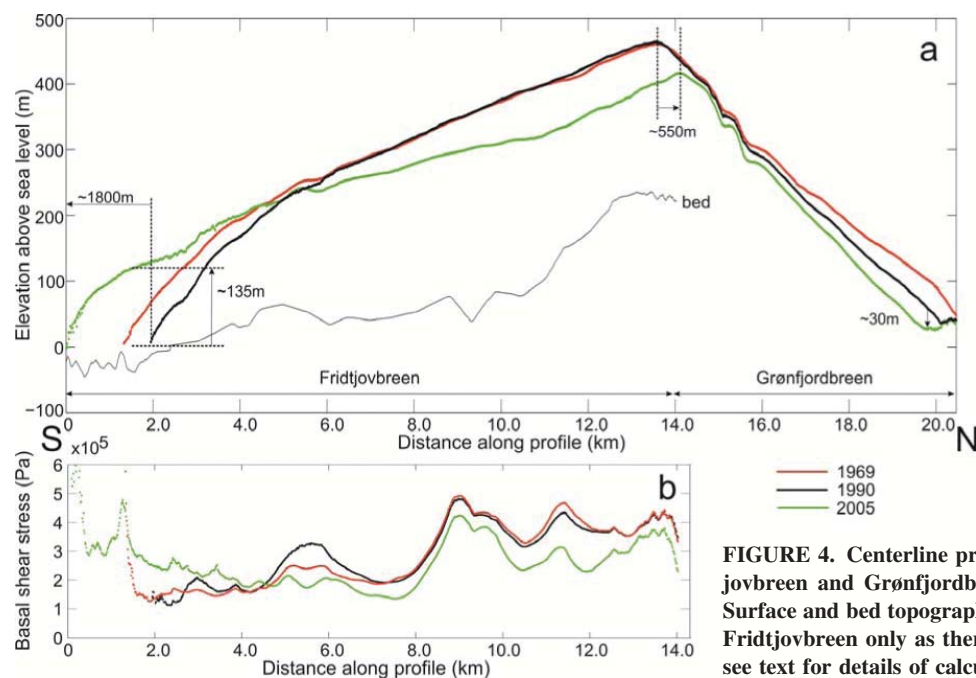
FIGURE 4. Centerline profiles from south to north along Fridt-jovbreen and Grønfjordbreen. Location shown in Figure 1. (a) Surface and bed topography. (b) Basal shear stress calculated for Fridtjovbreen only as there is no bed DEM for Grønfjordbreen; see text for details of calculation.
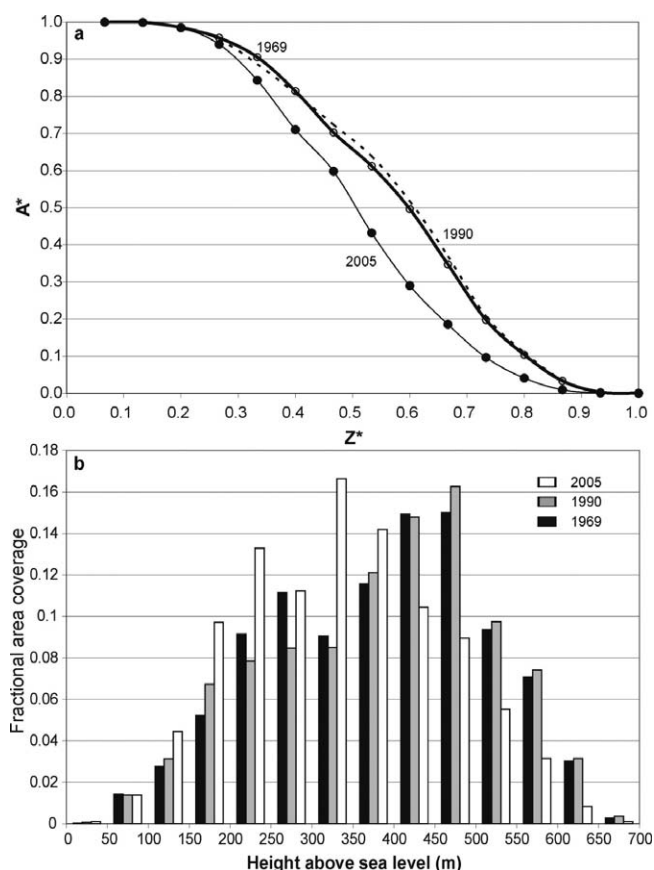
FIGURE 5. (a) Hypsometry for Fridtjovbreen at the different time epochs. A* and Z* are dimensionless area and elevation, respectively (e.g., Furbish and Andrews, 1984). A* is the cumulative area above a particular elevation. Z* is 0 at the glacier margin and 1 at the highest elevations. (b) Fraction of area of glacier in each elevation band in each time epoch.

In reporting the volume change of the glacier during the surge we have not made any correction for the increase in crevassing on the glacier during the surge. In a study of Sortebræ, east Greenland, Jiskoot et al. (2001) applied a volume correction in crevassed areas of ~10% to allow for this. The surface of Fridtjovbreen did become significantly crevassed during the surge (Murray et al., 2003a), which decreases the volume of ice stored in the post-surge glacier; however, the ice surface during a surge in Svalbard is less crevassed than occurs at Sortebræ, and any volume correction needed is un-likely to be as large as this. If we were to apply such a correction, this would increase the calculated volume of ice calved and hence rates of volume loss during the surge event. We have further as-sumed that the release of subglacially stored water does not contrib-ute to volume change significantly. This could be an important consideration if the glacier was fast flowing during any of the DEM collection epochs, as measurements at other glaciers show the ice surface can drop significantly at the end of the fast flow phase (Kamb et al., 1985). However, during 1990, flow rates at Fridtjov-breen had not accelerated, and by 2005, flow rates had dropped significantly and the margin was already in retreat, so this is un-likely to be a significant effect.

Discussion

An implication of the standard description of glacier surging is that surge behavior is a dynamic perturbation either side of equi-librium (flow being alternately too fast, too slow), and a glacier is assumed to return at the end of quiescence to its pre-surge geometry (see for example, discussions in van der Veen [1999], Benn and Evans [2010], and Cuffey and Paterson [2010]). However, in many surge clusters in the world, glacier mass balance is known to be negative. In western Svalbard, for example, Kohler et al. (2007) have shown that mass loss has been occurring at an accelerating

Tavi Murray et al. / 365

rate since the 1930s, and mass balance is likely to have been negative since the end of the Little Ice Age. Surges are common in this area even though the glaciers clearly cannot be returning to their original geometry after each event.

At Variegated Glacier, Alaska, surging appears to occur triggered by increases in glacier thickness (Eisen et al., 2001). However, at Fridtjovbreen crevassing on the glacier was first reported close to the front margin (A. J. Hodson, personal communication, 2002), where considerable thinning of the glacier was occurring. Remote sensing observations of flow during the early part of the surge show that fast flow started in the lower third of the glacier, and although the location cannot be better determined due to the limitations of SAR interferometry, fast flow clearly did not start at high elevation (Murray et al., 2003a). Furthermore, at the highest elevations, fast flow occurred first on the NW tributary, with the NE tributary, which is the part that thickened most in our measurements (the last 21 years of quiescence; Fig. 3, part a), speeding up only later in the surge (Murray et al., 2003a). Thus, on Fridtjovbreen it appears that the surge did not start in the upper part of the glacier, and certainly not in the region of greatest recent thickening (although note that the earlier measurements for 1936–1988 reported by Glazovsky et al. [1991] show the NW tributary thickening most). Kohler et al. (2007) reported that the glaciers and small ice cap they measured have been thinning at all elevations to 700 m a.s.l. since 1977. This is equivalent to the highest elevation on Fridtjovbreen (Fig. 5). Furthermore, in 1987–1988 the measured net mass balance on Fridtjovbreen was −0.37 m w.e. (Glazovsky et al., 1991). It therefore seems unlikely that the fast flow during Fridtjovbreen's surge was triggered by thickness changes, and increases in shear stress due to steepening (Fig. 4, part b) are more likely to be the cause. Steepening occurred mainly due to thinning in the lower glacier and retreat of the ice front rather than thickening of the upper glacier (Fig. 4 shows both Fridtjovbreen and Grønfjordbreen steepening, despite the latter thinning at all elevations). This pattern of steepening in profile of the lower glacier causing increased basal shear stresses (Fig. 4, part b) is consistent with the surge initiating in this region.

Dowdeswell et al. (1995) suggested that climate warming since the end of the Little Ice Age has reduced the number of glaciers that surge in the Svalbard archipelago due to two effects. The first is that reductions in mass balance will lengthen the time taken for a glacier to return to its pre-surge geometry. The second is that glacier geometries and regional climate changes favor transition to glaciers comprised entirely of cold-ice in Svalbard. This latter is almost certain to prevent a glacier being capable of surging, as sliding and sediment deformation are negligible beneath cold-ice, and no cold-based glacier has ever been observed to surge. However, as discussed above it is almost certain that most surge-type glaciers in Svalbard are not returning to their pre-surge geometry. If we are correct in our assertion that the surge at Fridtjovbreen was triggered by increasing shear stresses, changes in surface slope during the quiescent phase may allow glaciers in Svalbard to continue to surge despite their negative mass balances unless thinning causes them to become cold-based, or perhaps they retreat and become land-terminating. Indeed, the interval between successive surges could decrease as glaciers retreat if they also consequently steepen.

Conclusions

We have used geodetic methods to produce detailed surface DEMs at three time epochs that bracket fast flow during a surge event at Fridtjovbreen in central Spitsbergen. We used these in combination with a bed DEM to measure changes in ice volume, hypsometry, basal shear stress, and the volume of icebergs calved. The glacier lost ~5% of its volume during 21 years of quiescence despite some thickening in the reservoir zone. During the surge the glacier lost ~17.3% of its volume, with ~10.4% being calved as icebergs and the remaining ~6.8% running off as meltwater.

The overall volume of Fridtjovbreen has almost certainly been decreasing at an accelerating rate over the period we have studied. Despite this reduction in overall volume, the glacier surged in the 1990s. We therefore need to revise the notion that surging in this region is triggered by a return to an original geometry. In western Svalbard surges are superimposed on a more than 30 year trend of accelerating mass loss at elevations to at least 700 m a.s.l., so that it is unlikely that surges are triggered by the glacier reaching a certain thickness. We suggest that as a glacier progressively thins and shortens, changes in surface slope and consequent increases in basal shear stress trigger the surge.

References Cited

Bamber, J. L., Krabill, W., Raper, V., Dowdeswell, J. A., and Oerlemans, J., 2005: Elevation changes measured on Svalbard glaciers and ice caps from airborne laser data. *Annals of Glaciology*, 42: 202–208.

Barrand, N. E., Murray, T., James, T. D., Barr, S. L., and Mills, J. P., 2009: Optimizing photogrammetric DEMs for glacier volume change assessment using laser-scanning derived ground-control points. *Journal of Glaciology*, 55(189): 106–116.

Benn, D. I., and Evans, D. J. A., 2010: *Glaciers and Glaciation*. 2nd edition. London: Hodder Education, 802 pp.

Cuffey, K. M., and Paterson, W. S. B., 2010: *Physics of Glaciers*. 4th edition. Amsterdam: Elsevier, 693 pp.

Dowdeswell, J. A., Hodgkins, R., Nuttall, A. M., Hagen, J. O., and Hamilton, G. S., 1995: Mass-balance change as a control on the frequency and occurrence of glacier surges in Svalbard, Norwegian High Arctic. *Geophysical Research Letters*, 22(21): 2909–2912.

Eisen, O., Harrison, W. D., and Raymond, C. F., 2001: The surges of Variegated Glacier, Alaska, USA, and their connection to climate and mass balance. *Journal of Glaciology*, 47(158): 351–358.

Furbish, D. J., and Andrews, J. T., 1984: The use of hypsometry to indicate long-term stability and response of valley glaciers to changes in mass transfer. *Journal of Glaciology*, 30(105): 199–211.

Glasser, N. F., Huddart, D., and Bennett, M. R., 1998: Ice-marginal characteristics of Fridtjovbreen (Svalbard) during its recent surge. *Polar Research*, 17(1): 93–100.

Glazovsky, A. F., Ya, M. Y., and Yu, M. M., 1991: Tidewater glaciers of Spitsbergen. *In* Kotlyakov, V. M., Ushakov, A., and Glazovsky, A. (eds.), *Glaciers–Ocean–Atmosphere Interactions.* IASH Publ., 208: 229–239.

Hagen, J. O., Liestøl, O., Roland, E., and Jørgensen, T., 1993: *Glacier Atlas of Svalbard and Jan Mayen.* Oslo: Norsk Polarinstitutt, 141 pp.

Hjelle, A., Lauritzen, Ø., Salvigsen, O., and Winsnes, T. S., 1986: Geological Map of Svalbard 1:100,000 Sheet B10G Van Mijenfjorden. Oslo: Norsk Polarinstitutt, Temakart No. 2, with explanatory text, 37 pp.

James, T. D., Murray, T., Barrand, N. E., and Barr, S. L., 2006: Extracting photogrammetric ground control from lidar DEMs for change detection. *Photogrammetric Record*, 21(116): 312–328.

Jiskoot, H., Murray, T., and Boyle, P., 2000: Controls on the distribution of surge-type glaciers in Svalbard. *Journal of Glaciology*, 46(154): 412–422.

Jiskoot, H., Pedersen, A. K., and Murray, T., 2001: Multi-model photogrammetric analysis of the 1990s surge of Sortebrae, East Greenland. *Journal of Glaciology*, 47(159): 677–687.

Kamb, B., and Echelmeyer, K. A., 1986: Stress-gradient coupling in glacier flow: I. Longitudinal averaging of the influence of ice thickness and surface slope, *Journal of Glaciology*, 32(111): 267–284.

Kamb, B., Raymond, C. F., Harrison, W. D., Engelhardt, H., Echelmeyer, K. A., Humphrey, N., Brugman, M. M., and Pfeffer, T., 1985: Glacier surge mechanism—1982–1983 surge of Variegated Glacier, Alaska. *Science*, 227(4686): 469–479.

Kohler, J., James, T. D., Murray, T., Nuth, C., Brandt, O., Barrand, N. E., Aas, H. F., and Luckman, A., 2007: Acceleration in thinning rate on western Svalbard glaciers. *Geophysical Research Letters*, 34: L18502, http://dx.doi.org/10.1029/2007GL030681.

Kotlyakov, V. M., and Macheret, Y. Y., 1987: Radio-echo sounding of sub-polar glaciers: some problems and results of Soviet studies. *Annals of Glaciology*, 9151–9159.

Liljequist, G. H., 1993: *High Latitudes: a History of Swedish Polar Travels and Research.* Stockholm: Swedish Polar Research Secretariat in collaboration with Streiffert, 607 pp.

Luckman, A., Murray, T., and Strozzi, T., 2002: Surface flow evolution throughout a glacier surge measured by satellite radar interferometry. *Geophysical Research Letters*, 29(23): 2095, http://dx.doi.org/10.1029/2001GL014570.

Lønne, I., 2006: Low-velocity glacial surges—Processes unlocked by modern surge on Svalbard. *Geology*, 34(7): 553–556.

Macheret, Y. Y., and Glazovsky, A. F., 2000: Estimation of absolute water content in Spitsbergen glaciers from radar sounding data. *Polar Research*, 19(2): 205–216.

Mansell, D. T., Luckman, A., and Murray, T., 2012: Dynamics of tidewater surge-type glaciers in northwest Svalbard. *Journal of Glaciology*, 58(207): 110–118.

Murray, T., Dowdeswell, J. A., Drewry, D. J., and Frearson, I., 1998: Geometric evolution and ice dynamics during a surge of Bakaninbreen, Svalbard. *Journal of Glaciology*, 44(147): 263–272.

Murray, T., Luckman, A., Strozzi, T., and Nuttall, A. M., 2003a: The initiation of glacier surging at Fridtjovbreen, Svalbard. *Annals of Glaciology*, 36: 110–116.

Murray, T., Strozzi, T., Luckman, A., Jiskoot, H., and Christakos, P., 2003b: Is there a single surge mechanism? Contrasts in dynamics between glacier surges in Svalbard and other regions. *Journal of Geophysical Research–Solid Earth*, 108(B5): 2237, http://dx.doi.org/10.1029/2002JB001906.

Musial, A., 1994: Fridtjovbreen sediments and forms (West Spitsbergen). *In* Zalewski, S. M. (ed.), Proceedings of the XXI Polar Symposium, Warsaw, 149–157.

Muskett, R. R., Lingle, C. S., Sauber, J. M., Post, A. S., Tangborn, W. V., and Rabus, B. T., 2008: Surging, accelerating surface lowering and volume reduction of the Malaspina Glacier system, Alaska, USA, and Yukon, Canada, from 1972 to 2006. *Journal of Glaciology*, 54(188): 788–800.

Muskett, R. R., Lingle, C. S., Sauber, J. M., Post, A. S., Tangborn, W. V., Rabus, B. T., and Echelmeyer, K. A., 2009: Airborne and spaceborne DEM- and laser altimetry-derived surface elevation and volume changes of the Bering Glacier system, Alaska, USA, and Yukon, Canada, 1972–2006. *Journal of Glaciology*, 55(190): 316–326.

Nathorst, A. G., 1900: Två somrar i Norra Ishavet/Two summers in the Arctic Ocean, Parts I–II. Stockholm, 352 and 414 pp.

Norwegian Hydrographic Service, 1990: Den norske los. Arctic Pilot, Farvannsbeskrivelse (Sailing Directions), Svalbard and Jan Mayen, Volume 7. 2nd edition. Stavanger: Norwegian Hydrographic Service and Norwegian Polar Institute, 433 pp.

Pritchard, H., Murray, T., Strozzi, T., Barr, S., and Luckman, A., 2003: Surge-related topographic change of the glacier Sortebrae, East Greenland, derived from synthetic aperture radar interferometry. *Journal of Glaciology*, 49(166): 381–390.

Pritchard, H., Murray, T., Luckman, A., Strozzi, T., and Barr, S., 2005: Glacier surge dynamics of Sortebrae, east Greenland, from synthetic aperture radar feature tracking. *Journal of Geophysical Research–Earth Surface*, 110: F03005, http://dx.doi.org/10.1029/2004JF000233.

Raymond, C. F., 1987: How do glaciers surge—A review. *Journal of Geophysical Research–Solid Earth and Planets*, 92(B9): 9121–9134.

Shugar, D. H., Rabus, B. T., and Clague, J. J., 2010: Elevation changes (1949–1995) of Black Rapids Glacier, Alaska, derived from a multibaseline InSAR DEM and historical maps. *Journal of Glaciology*, 56(198): 625–634.

Strozzi, T., Luckman, A., Murray, T., Wegmuller, U., and Werner, C. L., 2002: Glacier motion estimation using SAR offset-tracking procedures. *IEEE Transactions on Geoscience and Remote Sensing*, 40(11): 2384–2391.

Sund, M., Eiken, T., Hagen, J. O., and Kääb, A., 2009: Svalbard surge dynamics derived from geometric changes. *Annals of Glaciology*, 50(52): 50–60.

van der Veen, C. J., 1999: *Fundamentals of Glacier Mechanics.* Rotterdam: AA Balkema, 462 pp.

Wilbur, S. W., 1988: Surging versus non-surging glaciers: a comparison using morphometry and balance. M.S. thesis, University of Alaska, Fairbanks, 113 pp.